MODEL VALIDATION OF A RESIDENTIAL SOLAR THERMAL COMBISYSTEM

Anthony Rey[1], Radu Zmeureanu[1]

[1]Centre for Zero Energy Building Studies, Department of Building, Civil and Environmental Engineering, Concordia University, Montreal, Quebec, Canada

an_rey@encs.concordia.ca radu.zmeureanu@concordia.ca

ABSTRACT

This paper presents the validation of a TRNSYS model of a residential solar thermal combisystem installed in the United States. This solar combisystem, installed in an occupied house, is composed of two distinct arrays of flat-plate collectors of 15.8 m^2 connected to a thermal storage tank of 617 liters, and provides for domestic hot water and space heating. The available measurements used for the model validation are from January to December 2014. The paper presents the system and uncertainty analysis of measurements. The main characteristics of the TRNSYS model are presented, followed by the comparison of the model predictions with the measurements of some selected variables of interest. For instance, the coefficient of variation of root-mean-squared error (CVRMSE) for the measured temperatures ranged from 8.6% to 25.1%.

INTRODUCTION

The building sector accounts for over one-third of total final energy consumption in the world, and its energy demand could rise by 50% by 2050 if no action is taken (IEA, 2013). Solar energy appears to be one of the most suitable renewable energy sources for residential buildings. Its most common use is for the direct heating of air and water (Nyboer and Lutes, 2011), which is why solar water heating (SWH) is the most widely used solar energy application in the world (Mauthner and Weiss, 2013). Solar water heaters are therefore a viable alternative to reduce fossil fuel consumption and greenhouse gas emissions of residential buildings (Kalogirou, 2004). Although an increasing interest in SWH systems has emerged over the last 20 years (Hang, Qu, and Zhao, 2012), priority should be given to solar thermal combisystems, since they are more environmentally-friendly (Bornatico, et al., 2012). Solar combisystems provide energy for both domestic hot water (DHW) and space heating (SH) needs. Since the late 90s, several research studies have been conducted on solar combisystems. The Solar heating and Cooling (SHC) Programme has even devoted one of its projects to solar combisystems (IEA, 2015). Task 26 was a comprehensive project performed by a group of 35 experts and 16 solar industries from nine European countries and the USA, from 1998 to 2002 to investigate solar combisystems (Suter, Weiss, and Inäbnit, 2000). From 2001 to 2003, the European Alterner Programme Project studied more than 200 solar combisystems installed in seven European countries (Ellehauge, 2015). As mentioned in (Hugo, Zmeureanu, and Rivard, 2010), the market penetration of solar thermal systems significantly varies between Europe and North America. It was noted in (Dickinson and Cruickshank, 2011) that little research has been conducted on residential solar combisystems in North America.

Most research studies were conducted by using building performance simulation (BPS) programs, but only a few were related to existing solar combisystems. In addition, a lack of uncertainty analysis associated with building performance simulations was reported in (Attia et al., 2013). It was also pointed out in (Coakley, Raftery, and Keane, 2014) that calibration is often not considered in research studies. A few examples of solar combisystem related research efforts are discussed herein. The life cycle cost and energy analysis of a simulation-based net zero energy house (NZEH) using a solar combisystem was studied in (Leckner and Zmeureanu, 2011). An energy analysis of an experimental solar combisystem located in Turkey was performed in (Kacan and Ulgen, 2012). In (Bornatico, et al., 2012), an optimization of a simulation-based solar combisystem was performed using Vela Solaris Polysun (Polysun, 2015) and MATLAB (MATLAB, 2015). The same model was optimized using a surrogate model in (Bornatico, et al., 2013). An analysis and optimization of a solar combisystem using a carbon dioxide heat pump was executed in (Deng, Dai, and Wang, 2013), using TRNSYS (TRNSYS, 2015). A solar combisystem installed in a detached house, occupied by a four-member family, was simulated with a BPS software in

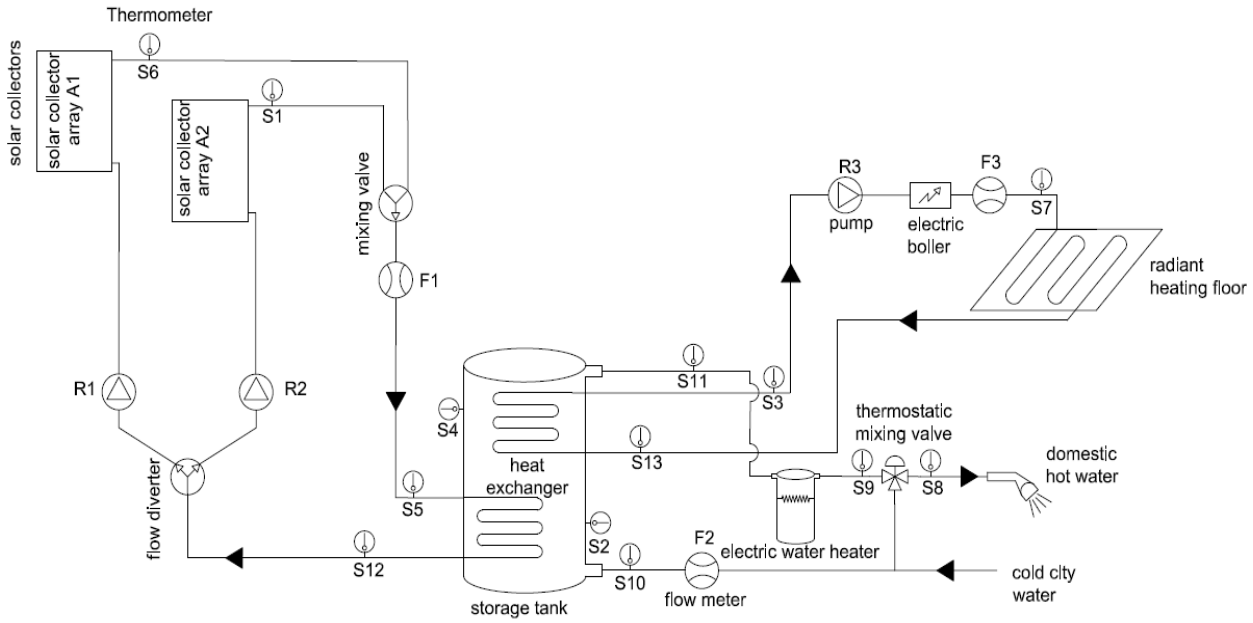

Figure 1. Scheme of the monitored solar thermal combisystem

(Martinopoulos and Tsalikis, 2014). Another simulation-based solar combisystem implemented in TRNSYS was optimized in (Ng Cheng Hin and Zmeureanu, 2014).

This literature review revealed that most research studies about solar combisystems used BPS programs to model generic systems. The model validation and uncertainty analysis were not conducted on existing solar thermal combisystems. This paper presents the validation of a TRNSYS model of a residential solar combisystem installed in Massachusetts, USA.

SYSTEM DESCRIPTION

Through the collaboration of a leading international manufacturer of SWH technologies, measurements from this existing solar combisystem were obtained between January 2014 and January 2015. The solar thermal combisystem is designed to supply both DHW and SH needs. As illustrated in Figure 1, the solar combisystem is composed of two distinct arrays of three flat-plate collectors (FPCs) each, giving a total of six solar thermal collectors. Both arrays of solar thermal collectors (i.e., arrays A1 and A2) are south-facing, but have two distinct tilt angles equal to 65° and 90° above the horizontal, respectively. Solar energy is harvested by a heat-transfer fluid, which is a 40% glycol-water mixture, circulated by pumps through the solar collectors. One storage tank, which allows solar energy to be stored, is used for both domestic hot water and space heating needs. Additional energy is provided, when it is required, by an electrical boiler for the radiant floor and by an electrical heater for domestic hot water. Temperature sensors and flow meters have been installed at the locations indicated in Figure 1. Measurements are recorded every minute, and the average values are calculated to provide other data resolutions: five-minute interval, hourly, and daily.

This study uses hourly values, unless otherwise stated. Table 1 lists all the available sensors. It should be noted that the mass flow rates are provided in L/min, but were converted to kg/s in this study, unless otherwise stated. The solar thermal combisystem is installed in a house of approximately 110 m^2, inhabited by a family. There is no detailed information about the house nor about the energy-related people's behavior. The outside air temperature and solar radiation were not measured on site during the studying period; they were obtained for the year 2014 from Weather Analytics (Weather Analytics, 2015). Weather Analytics uses the Climate Forecast System Reanalysis (CFSR) data set, which estimates the outside air temperature and solar radiation based on a full atmospheric model using observational data and past model verifications.

ENERGY PERFORMANCE INDICES

Two performance indices are selected to assess the energy performance of the solar combisystem:

(i) Thermal efficiency of the solar collectors;
(ii) Thermal energy stored in the storage tank.

Table 1. List of the sensors monitoring the residential solar thermal combisystem

Sensor	Measured physical quantity	Unit
S1	Outlet heat-transfer fluid temperature of A2 array	°C
S2	Water temperature of the lower part of the storage tank	°C
S3	Water temperature going to the radiant floor	°C
S4	Water temperature of the upper part of the storage tank	°C
S5	Average heat-transfer fluid temperature leaving both arrays of solar collectors	°C
S6	Outlet heat-transfer fluid temperature of A1 array	°C
S7	Supply water temperature for the radiant floor	°C
S8	Supply DHW temperature	°C
S9	DHW temperature leaving the electrical water heater	°C
S10	Temperature of the cold city water	°C
S11	DHW temperature leaving the thermal storage tank	°C
S12	Heat-transfer fluid temperature entering the solar thermal collectors	°C
S13	Return water temperature from the radiant floor	°C
F1	Heat-transfer fluid mass flow rate through the solar collectors	L/min
F2	Cold city water mass flow rate entering the storage tank	L/min
F3	Water mass flow rate through the radiant floor	L/min

ENERGY PERFORMANCE INDICES

Two performance indices are selected to assess the energy performance of the solar combisystem:

(iii) Thermal efficiency of the solar collectors;
(iv) Thermal energy stored in the storage tank.

The thermal efficiency of the solar collectors is calculated as follows (Duffie and Beckman, 2006):

$$\eta_{coll} = \frac{\dot{Q}_{harvested,coll}}{\dot{Q}_{received,coll}} \cdot 100 = \frac{\dot{m}_{coll} \cdot c_{p,coll} \cdot (T_{S5} - T_{S12})}{A_{A1} \cdot G_{T,A1} + A_{A2} \cdot G_{T,A2}} \cdot 100 \quad (1)$$

where $\dot{Q}_{harvested,coll}$ is the rate of heat harvested by the solar collector [W]; $\dot{Q}_{received,coll}$ is the rate of solar energy received by the solar collector [W]; $\dot{m}_{coll}$ is the heat-transfer fluid mass flow rate [kg/s]; $c_{p,coll}$ is the specific heat of the heat-transfer fluid [J/(kg.°C)]; T_{S5} and T_{S12} are the outlet and inlet average heat-transfer fluid temperatures of the solar collector arrays [°C], respectively; A_{A1} and A_{A2} are the gross areas of the solar collector arrays A1 and A2 [m^2], respectively; $G_{T,A1}$ and $G_{T,A2}$ are the total solar irradiances incident on the solar collector arrays A1 and A2 [W/m^2], respectively.

Since the thermal storage tank is not equipped with any electric heater, its thermal energy stored, Q_{stored}, is calculated as follows:

$$Q_{stored} = Q_{supply} - (Q_{DHW} + Q_{SH}) \quad (2)$$

where:

$$Q_{supply} = \Delta t \cdot \dot{m}_{coll} \cdot c_{p,coll} \cdot (T_{S5} - T_{S12}) \quad (3)$$

$$Q_{DHW} = \Delta t \cdot \dot{m}_{DHW} \cdot c_{p,w} \cdot (T_{S11} - T_{S10}) \quad (4)$$

$$Q_{SH} = \Delta t \cdot \dot{m}_{SH} \cdot c_{p,w} \cdot (T_{S3} - T_{S13}) \quad (5)$$

where Q_{supply} is the solar energy supplied to the thermal storage tank [kWh]; Q_{DHW} and Q_{SH} are the amounts of energy supplied by the tank for domestic hot water and space heating [kWh], respectively; Δt is the time step between two measurements [h]; $\dot{m}_{DHW}$ and $\dot{m}_{SH}$ are the water mass flow rates for DHW and SH [kg/s], respectively; $c_{p,w}$ is the specific heat of water [kJ/(kg.°C)]; T_{S11} and T_{S10} are the temperatures of the DHW leaving and entering the thermal storage tank [°C], respectively; T_{S3} and T_{S13} are the temperatures of the water leaving and entering the internal heat exchanger within the thermal storage tank for spacing heating [°C], respectively.

UNCERTAINTY ANALYSIS

Data collection provides valuable insights; however, the misuse of data can lead to false conclusions. As mentioned in (Reddy, 2011), measurements made in the field are more subject to errors than the ones made under the controlled conditions of a laboratory setting. Uncertainty arises from any measurement, and therefore the uncertainty analysis is necessary to assess their impact on the estimates of the energy performance indicators. Errors in measurements can be separated into two parts: (i) bias errors, and (ii) random errors.

Overall uncertainty

Bias errors, also called systematic errors, are fixed values. They are provided by manufacturers at a specified confidence level. Random errors are non-repeatable inaccuracies, which can be estimated by repeating a measurement. Any measurement of a variable x can be defined as follows:

$$x = x_{best} \pm U_x \tag{6}$$

where x_{best} is the best estimate of the variable x (i.e., the measured value); U_x is the overall uncertainty in the measurement.

The overall uncertainty of a measured variable x, at a specified confidence, combines the random and bias uncertainty estimates, and is expressed as (Reddy, 2011):

$$U_x = \sqrt{{B_x}^2 + \left(\frac{t \cdot s_x}{\sqrt{n}}\right)^2} \tag{7}$$

where B_x is the uncertainty in the bias component; s_x is the standard deviation estimates for the random component; n is the sample size; t is the t-value at the specified confidence level for the appropriate degrees of freedom.

Propagation of errors

Assuming a variable y depending on n measured variables x such that:

$$y = f(x_1, \dots, x_n) \tag{8}$$

The overall uncertainty in y is calculated using the general formula for error propagation as follows (Reddy, 2011):

$$U_y = \sqrt{\left(\frac{\partial y}{\partial x_1} \cdot U_{x1}\right)^2 + \cdots + \left(\frac{\partial y}{\partial x_n} \cdot U_{xn}\right)^2} \tag{9}$$

where U_{xi} is the overall uncertainty in the i-th measured variables x, calculated using Equation 7.

Equation 9 is applied to the two energy performance indicators to estimate their respective overall uncertainty. The overall uncertainty in η_{coll} is determined as shown in Equation 10:

$$U_{\eta_{coll}} = \left[\begin{array}{l}\left(\frac{\partial \eta_{coll}}{\partial \dot{m}_{coll}} \cdot U_{\dot{m}_{coll}}\right)^2 + \left(\frac{\partial \eta_{coll}}{\partial c_{p,coll}} \cdot U_{c_{p,coll}}\right)^2 + \left(\frac{\partial \eta_{coll}}{\partial T_{S5}} \cdot U_{T_{S5}}\right)^2 + \left(\frac{\partial \eta_{coll}}{\partial T_{S12}} \cdot U_{T_{S12}}\right)^2 \\ + \left(\frac{\partial \eta_{coll}}{\partial A_{A1}} \cdot U_{A_{A1}}\right)^2 + \left(\frac{\partial \eta_{coll}}{\partial A_{A2}} \cdot U_{A_{A2}}\right)^2 + \left(\frac{\partial \eta_{coll}}{\partial G_{T,A1}} \cdot U_{G_{T,A1}}\right)^2 + \left(\frac{\partial \eta_{coll}}{\partial G_{T,A2}} \cdot U_{G_{T,A2}}\right)^2\end{array}\right]^{1/2} \tag{10}$$

Since the outside air temperature and solar radiation were not measured on site, the uncertainties related to the measurements of $G_{T,A1}$ and $G_{T,A2}$ are neglected. . The uncertainty in the specific heat of the 40% glycol-water heat-transfer fluid is also neglected. Assuming that the uncertainty in the measured areas is negligible, the overall uncertainty in η_{coll} is calculated as follows:

$$U_{\eta_{coll}} = \left[\begin{array}{l}\left(\frac{\partial \eta_{coll}}{\partial \dot{m}_{coll}} \cdot U_{\dot{m}_{coll}}\right)^2 \\ + \left(\frac{\partial \eta_{coll}}{\partial T_{S5}} \cdot U_{T_{S5}}\right)^2 \\ + \left(\frac{\partial \eta_{coll}}{\partial T_{S12}} \cdot U_{T_{S12}}\right)^2\end{array}\right]^{1/2} \tag{11}$$

where:

$$\frac{\partial \eta_{coll}}{\partial \dot{m}_{coll}} = \frac{c_{p,coll} \cdot (T_{S5} - T_{S12})}{A_{A1} \cdot G_{T,A1} + A_{A2} \cdot G_{T,A2}} \tag{12}$$

$$\frac{\partial \eta_{coll}}{\partial T_{S5}} = \frac{\dot{m}_{coll} \cdot c_{p,coll}}{A_{A1} \cdot G_{T,A1} + A_{A2} \cdot G_{T,A2}} \tag{13}$$

$$\frac{\partial \eta_{coll}}{\partial T_{S12}} = -\frac{\dot{m}_{coll} \cdot c_{p,coll}}{A_{A1} \cdot G_{T,A1} + A_{A2} \cdot G_{T,A2}} \tag{14}$$

The overall uncertainty in the thermal energy stored in the storage tank is determined as follows:

$$U_{Q_{stored}} = \sqrt{{U_{Q_{supply}}}^2 + {U_{Q_{DHW}}}^2 + {U_{Q_{SH}}}^2} \tag{15}$$

in which:

$$U_{Q_{supply}} = \left[\begin{array}{l}\left(\frac{\partial \dot{Q}_{supply}}{\partial \dot{m}_{coll}} \cdot U_{\dot{m}_{coll}}\right)^2 \\ + \left(\frac{\partial \dot{Q}_{supply}}{\partial T_{S5}} \cdot U_{T_{S5}}\right)^2 \\ + \left(\frac{\partial \dot{Q}_{supply}}{\partial T_{S12}} \cdot U_{T_{S12}}\right)^2\end{array}\right]^{1/2} \tag{16}$$

$$U_{Q_{DHW}} = \left[\begin{array}{l} \left(\frac{\partial Q_{DHW}}{\partial \dot{m}_{DHW}} \cdot U_{\dot{m}_{DHW}}\right)^2 \\ + \left(\frac{\partial Q_{DHW}}{\partial T_{S11}} \cdot U_{T_{S11}}\right)^2 \\ + \left(\frac{\partial Q_{DHW}}{\partial T_{S10}} \cdot U_{T_{S10}}\right)^2 \end{array} \right]^{1/2} \quad (17)$$

$$U_{Q_{SH}} = \left[\begin{array}{l} \left(\frac{\partial Q_{SH}}{\partial \dot{m}_{SH}} \cdot U_{\dot{m}_{SH}}\right)^2 \\ + \left(\frac{\partial Q_{SH}}{\partial T_{S3}} \cdot U_{T_{S3}}\right)^2 \\ + \left(\frac{\partial Q_{SH}}{\partial T_{S13}} \cdot U_{T_{S13}}\right)^2 \end{array} \right]^{1/2} \quad (18)$$

where:

$$\frac{\partial \dot{Q}_{supply}}{\partial \dot{m}_{coll}} = c_{p,coll} \cdot (T_{S5} - T_{S12}) \quad (19)$$

$$\frac{\partial \dot{Q}_{supply}}{\partial T_{S5}} = \dot{m}_{coll} \cdot c_{p,coll} \quad (20)$$

$$\frac{\partial \dot{Q}_{supply}}{\partial T_{S12}} = -\dot{m}_{coll} \cdot c_{p,coll} \quad (21)$$

$$\frac{\partial Q_{DHW}}{\partial \dot{m}_{DHW}} = c_{p,water} \cdot (T_{S11} - T_{S10}) \quad (22)$$

$$\frac{\partial Q_{DHW}}{\partial T_{S11}} = \Delta t \cdot \dot{m}_{DHW} \cdot c_{p,w} \quad (23)$$

$$\frac{\partial Q_{DHW}}{\partial T_{S10}} = -\Delta t \cdot \dot{m}_{DHW} \cdot c_{p,w} \quad (24)$$

$$\frac{\partial Q_{SH}}{\partial \dot{m}_{SH}} = c_{p,w} \cdot (T_{S3} - T_{S13}) \quad (25)$$

$$\frac{\partial Q_{SH}}{\partial T_{S3}} = \Delta t \cdot \dot{m}_{SH} \cdot c_{p,w} \quad (26)$$

$$\frac{\partial Q_{SH}}{\partial T_{S13}} = -\Delta t \cdot \dot{m}_{SH} \cdot c_{p,w} \quad (27)$$

Uncertainty calculations

In order to estimate the overall uncertainty in the thermal efficiency of the solar collectors and thermal energy stored in the storage tank, the bias and random errors in each physical variable needs to be known. Random errors are unpredictable differences from one measurement to the next one due to unknown effects. They can be estimated through statistical analysis by repeating the same measurement as many times as possible. In most cases, it is impractical to perform the same measurement several times. Besides, the measured data of the solar thermal combisystem depend on external conditions that cannot be controlled, such as the outside temperature. In this study, 278 small samples of 31 measurements with the shortest time interval available (i.e., one minute between two measurements) are selected. By selecting such a sample, one can assume that environmental conditions do not significantly vary during each selected time period. The standard deviation of each sample s_x is calculated as follows:

$$s_x = \frac{1}{n-1} \cdot \sum_{i=1}^{n} (x_i - \bar{x})^2 \quad (28)$$

where n is the sample size; x_i is the i-th measurement; $\bar{x}$ is the arithmetic mean.

Since the measurements can be either higher or lower than the arithmetic mean, the *t*-value is the critical value for a two-tailed confidence level. For a degree of freedom equal to 30 and a specified confidence level of 95% (i.e., α equal to 0.05), the *t*-value is equal to 2.042 (Reddy, 2011). The average random error of each physical variable is estimated for the time interval November 17 to November 22, 2014. This time frame is chosen, because both the DHW and radiant floor were used by the people living in the house. Table 2 reports the bias error as well as the average random errors in the measurements over the 278 samples.

The average overall uncertainty of the two performance indices η_{coll} and $U_{Q_{stored}}$ from November 17 to November 22, 2014 are equal to 1% and 1.48 kWh, respectively.

MODEL PRESENTATION

The model of residential solar thermal combisystem was developed in the TRNSYS 17 simulation environment (see Figure 2). TRNSYS allows linking system components together, so as to simulate the thermal performance of complex energy systems. System components, also referred to as types, are Fortran-based subroutine having inputs and outputs.

Table 2. Bias and average random errors in the measurements from November 17 to November 22, 2014

Sensor	Bias error	Average random error	Unit
Temperature sensor			
S1	± 0.3 + 0.005· $\|T\|$	± 0.26	°C
S2	± 0.3 + 0.005· $\|T\|$	± 0.10	°C
S3	± 0.3 + 0.005· $\|T\|$	± 0.17	°C
S4	± 0.3 + 0.005· $\|T\|$	± 0.15	°C
S5	± 0.3 + 0.005· $\|T\|$	± 0.18	°C
S6	± 0.3 + 0.005· $\|T\|$	± 0.28	°C
S7	± 0.3 + 0.005· $\|T\|$	± 0.30	°C
S8	± 0.3 + 0.005· $\|T\|$	± 0.20	°C
S9	± 0.3 + 0.005· $\|T\|$	± 0.34	°C
S10	± 0.3 + 0.005· $\|T\|$	± 0.64	°C
S11	± 0.3 + 0.005· $\|T\|$	± 0.24	°C
S12	± 0.3 + 0.005· $\|T\|$	± 0.14	°C
S13	± 0.3 + 0.005· $\|T\|$	± 0.26	°C
Flowmeter			
F1 (solar loop)	± 5%	± 0.00036	kg/s
Flowmeter			
F2 (DHW loop)	± 5%	± 0.00036	kg/s
F3 (SH loop)	± 5%	± 0.00036	kg/s

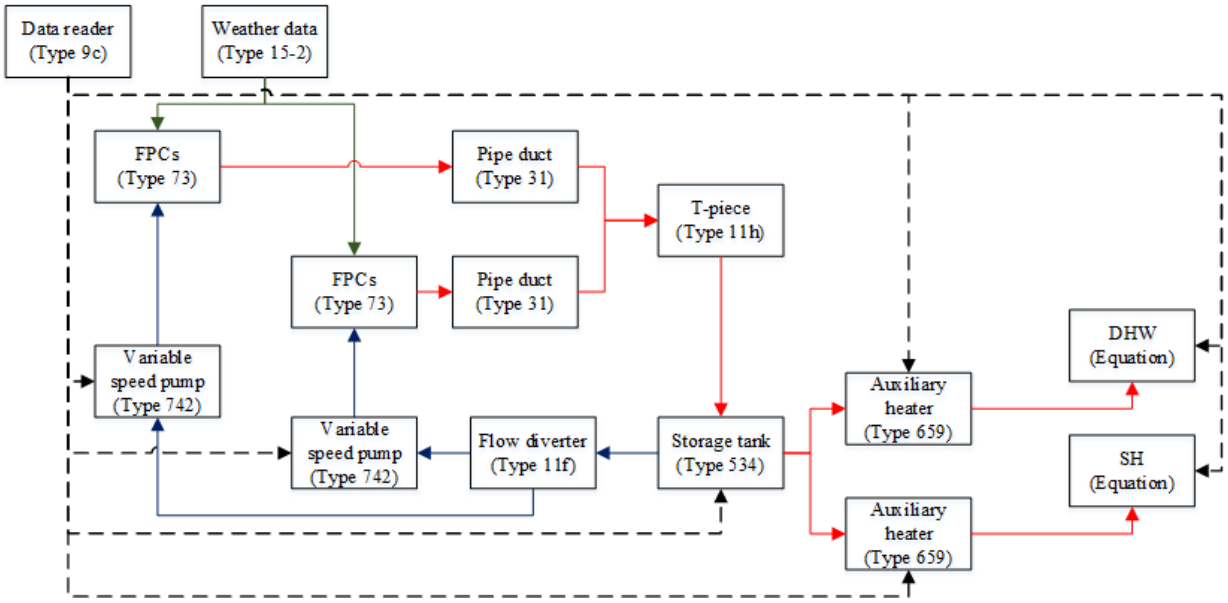

Figure 2. Flow diagram for the TRNSYS solar combisystem model

The two main components of this TRNSYS model are:

(i) The flat-plate collectors (Type 73);
(ii) The thermal storage tank (Type 534).

Flat-plate collectors: Type 73

Type 73 was used to simulate the two arrays of solar flat-plate collectors. Type 73 is based on the steady-state Hottel-Whiller analysis to calculate the solar thermal efficiency as follows (Duffie and Beckman, 2006):

$$\eta = a_0 - a_1 \cdot \frac{(T_{in} - T_a)}{G_T} - a_2 \cdot \frac{(T_{in} - T_a)}{G_T} \quad (29)$$

where η is the flat-plate collector efficiency [-]; a_0 is the optical efficiency [-]; a_1 is the first-order heat loss coefficient [W/(m^2.°C)]; a_2 is the second-order heat loss

Table 3.Some parameters for the flat-plate solar collectors

Parameter	FPC (Array A1)	FPC (Array A2)	Unit
Gross area per solar collector	2.70	2.54	m^2
Absorber area per solar collector	2.50	2.38	m^2
Fluid specific heat	3.7	3.7	kJ/(kg.°C)
Optical efficiency a_0	0.78	0.82	-
First-order heat loss coefficient a_1	2.84	3.46	W/(m^2.°C)
Second-order heat loss coefficient a_2	0.0154	0.0153	W/(m^2.°C^2)
Solar collector slope	65	90	Degrees

Table 4. Some parameters for the thermal storage tank

Parameter	FPC (Array A1)	Unit
Number of tank nodes	10	-
Tank volume	0.617	m^3
Tank height	1.67	m
Node height	0.0835	m
Fluid specific heat	4.19	kJ/kg.K
Fluid density	1000	kg/ m^3

coefficient [W/(m^2.°C^2)]; T_{in} and T_a are the inlet heat-transfer fluid and ambient temperatures [°C], respectively; G_T is the total solar irradiance incident on the solar collector [W/m^2]. Table 3 reports some of the main parameters used in Type 73. Since the solar combisystem is composed of two distinct arrays of three solar thermal collectors, different parameters are used for each type of flat-plate collector.

Thermal storage tank: Type 534

The thermal storage tank of 617 liters, was modeled using Type 534 (TESS, 2012). Type 534 models a vertically cylindrical stratified tank using a multi-node approach (see Table 4). The thermal storage tank is divided into N ($N \leq 20$) constant volume sections, called nodes, with node 1 at the top and node N at the bottom. The water of each node is assumed to be fully mixed and at a uniform temperature.

Data reader: Type 9c

The data reader reads from a text file some measurements of the existing solar combisystem, which are then used as inputs to the model. Thus, the cold city water mass flow rate and temperature entering the storage tank, as well as the water mass flow rate and return water temperature from the radiant floor are provided to Type 534 by using the data reader. The DHW temperature leaving the storage tank T_{11} and SH water temperature leaving the storage tank for the radiant floor $T_3$are predicted. Afterwards, the measured and simulated data can be compared to validate the residential solar thermal combisystem.

MODEL VALIDATION

Forward models (ASHRAE, 2013) use physical characteristics of a system as inputs, whereas inverse models are developed with measurements from a system. Models developed using BPS programs are forward models. As mentioned in (Coakley, Raftery, and Keane, 2014), significant differences can occur between the measurements from the system and the prediction of BPS models if a calibration is not accomplished. Calibration aims at reducing the discrepancies between model outputs and measured data to achieve more reliable results. As a result, a model can be considered validated when the acceptance criteria for calibration are fulfilled.

There are two main calibration issues are:

(i) Lack of explicit standards;
(ii) Large amount of model inputs compared to measurable outputs.

Lack of explicit standards

Acceptance criteria for calibration of buildings are given in (ASHRAE, 2002) and (EVO, 2007). Both use the normalized mean bias error (NMBE) and coefficient of variation of the root mean square deviation (CVRMSE) defined by Equations 30 and 31. However, as reported in Table 5, they do not recommend the same values. Although acceptance criteria for the calibration of the whole building energy use exist, there is no standard for the calibration of solar thermal combisystems.

Table 5. Acceptance criteria for the calibration of the whole building energy use

Standard/Guideline	Monthly criteria [%]		Hourly criteria [%]	
	NMBE	CVRMSE	NMBE	CVRMSE
ASHRAE Guideline 14 (ASHRAE, 2002)	5	15	10	30
IPMVP (EVO, 2007)	20	-	5	20

For instance, variations between predicted and measured values were quantified in (Ayompe et al., 2011) using percentage mean absolute error (PMAE) and percentage mean error (PME), instead of NMBE and CVRSME. The same criteria were also used in (Abdalla, 2013) to validate a solar water heating system model, where the PMAE for solar fraction was equal to 10% for example.

Large amount of model inputs compared to measurable outputs

Many inputs are required in order to develop the solar thermal combisystem model. Some data are difficult to obtain from manufacturers and others come with a certain uncertainty. As a result, BPS models encounter various sources of uncertainty (De Wit and Augenbroe, 2002).

Validation procedure

In order to validate the BPS model of this residential solar combisystem, four metrics are used: (i) normalized mean bias error (NMBE), (ii) coefficient of variation of the root mean square deviation (CVRMSE), (iii) percentage mean absolute error (PMAE), and (iv) percentage mean error (PME). The NMBE is calculated as follows (ASHRAE, 2002):

$$NMBE = \frac{\sum_{i=1}^{n}(y_i - \hat{y}_i)}{(n-p)\cdot \bar{y}} \cdot 100 \quad (30)$$

where y_i is the i-th variable observation; $\hat{y}_i$ is the i-th simulation-predicted value of the observed variable; n is the number of variable observations; p is the degree of freedom; $\bar{y}$ is the arithmetic mean of the variable observations. The CVRMSE is a normalized measure of dispersion, which is defined as follows as (ASHRAE, 2002):

$$CVRMSE = \frac{RMSE}{\bar{y}} \cdot 100 \quad (31)$$

where RMSE is the root-mean-square error calculated as (ASHRAE, 2002):

$$RMSE = \sqrt{\frac{\sum_{i=1}^{n}(y_i - \hat{y}_i)^2}{(n-p)}} \quad (32)$$

Table 6. Statistical indices comparing predicted with measured data of the solar combisystem for the year 2014

Sensor/Indicator	NBME [%]	CVRMSE [%]	PMAE [%]	PME [%]
Temperature				
S1	-0.7	11.4	5.4	2.7
S2	8.7	24.3	20.7	-1.6
S3	4.1	10.5	6.0	-3.4
S4	9.1	25.1	21.7	-2.4
S5	-0.8	13.5	5.0	1.5
S6	2.4	12.6	8.4	2.4
S9	6.2	25.0	23.7	1.7
S11	-0.1	8.6	3.19	1.0
S12	-2.1	14.3	6.0	3.8
Performance indices				
η_{coll}	7.3	29.3	25.0	18.7
Q_{supply}	-0.3	27.5	29.6	19.6
Q_{DHW}	3.2	21.3	25.6	4.4
Q_{SH}	2.1	14.8	1.2	1.1
Q_{stored}	7.6	35.5	21.4	5.5

The PMAE and PME are calculated as follows (Ayompe et al., 2011):

$$PMAE = \frac{100}{n} \cdot \sum_{i=1}^{n} \frac{|\hat{y}_i - y_i|}{y_i} \quad (33)$$

$$PME = \frac{100}{n} \cdot \sum_{i=1}^{n} \frac{\hat{y}_i - y_i}{y_i} \quad (34)$$

Although there is no standard for the calibration of solar thermal combisystems, the order of magnitude given for the first two metrics in (ASHRAE, 2002) and (EVO, 2007) are taken as a relative reference for the validation.

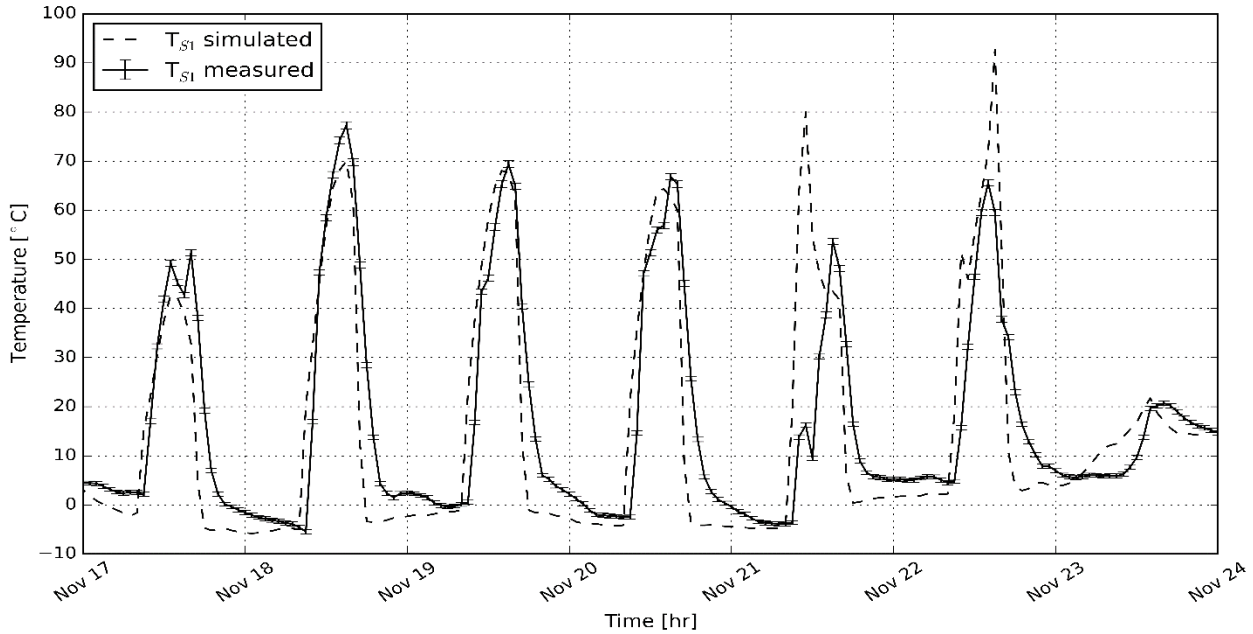

(b) Heat-transfer fluid temperature T_{S1} of the array A2

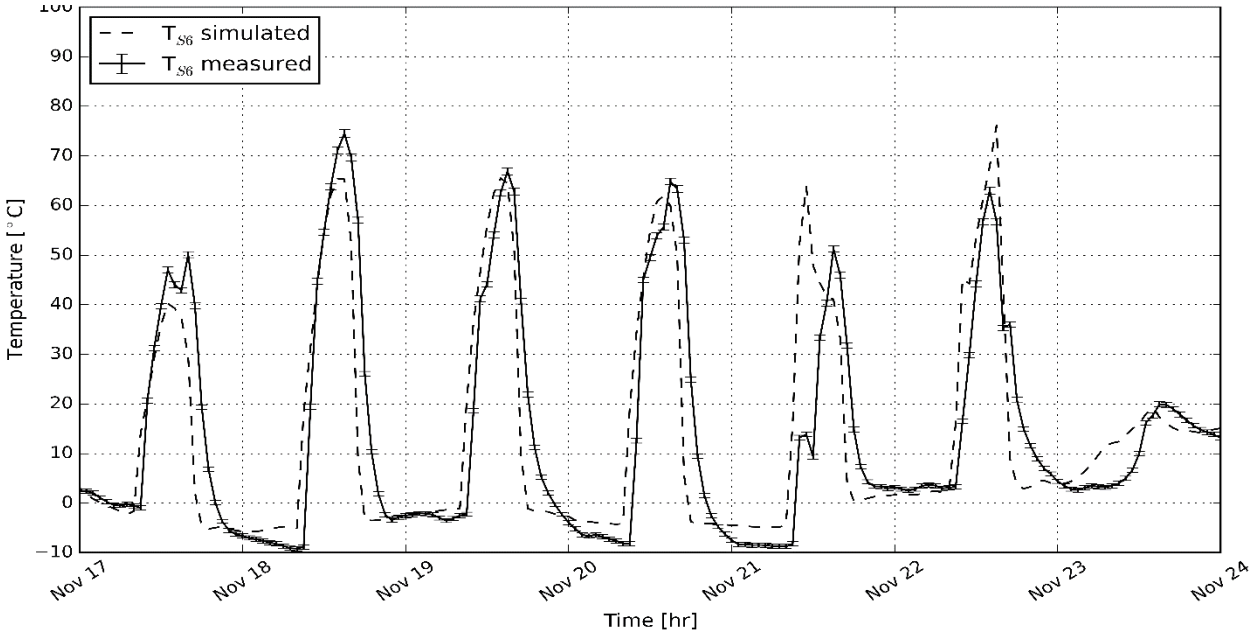

(a) Heat-transfer fluid temperature T_{S6} of the array A1

Figure 3. Comparison of the measured and simulated heat-transfer fluid temperatures leaving both the array A1 and A2 from November 17 to November 23, 2014

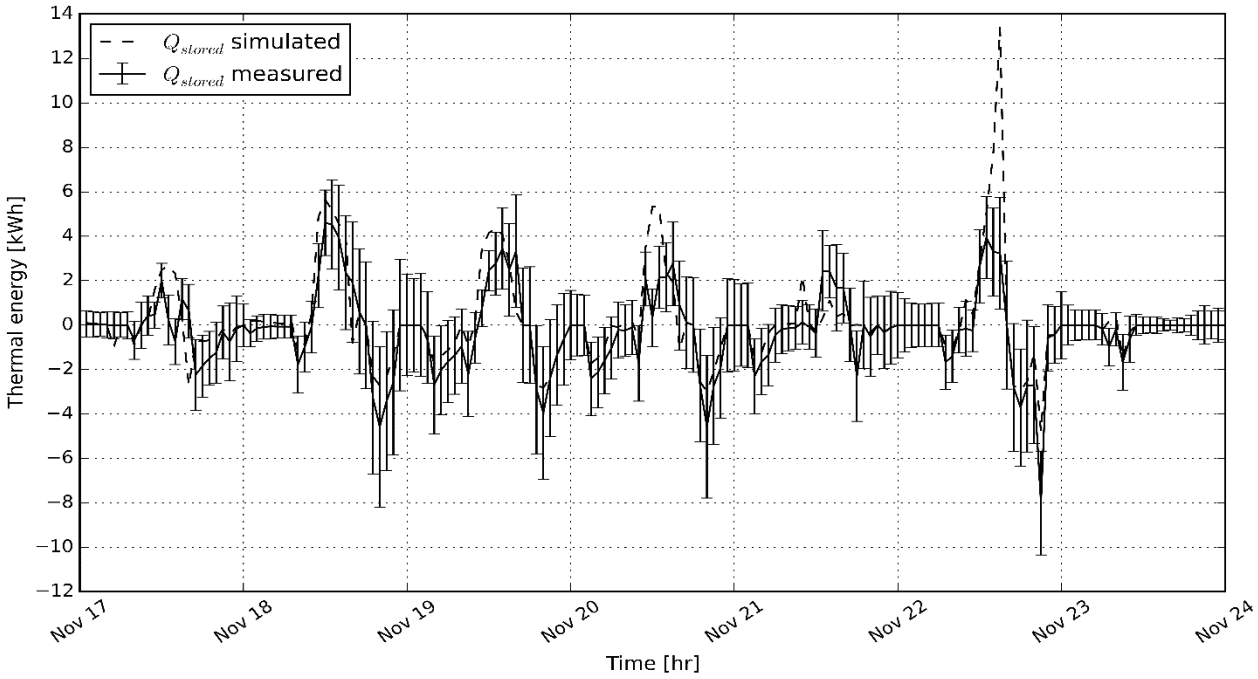

Figure 4. Comparison of the measured and simulated thermal energy stored in the storage tank from November 17 to November 23, 2014

Each metric is applied to some of the monitored temperatures as well as the two energy performance indicators, as shown in Table 6. Due to space limitations, only a few comparisons are reported herein. Figures 3 and 4 show the measured and predicted temperatures leaving the two solar thermal collector arrays A1 and A2, and thermal energy stored in the storage tank, respectively.

The simulated temperatures fit relatively well the measurements, which gives confidence about the model validation. However, larger discrepancies occur between the measured and simulated values of the performance indices. As shown in Figure 4, the propagation of errors for the estimation of heat flows is greater than the uncertainty of the measured temperatures (see Table 2).

Table 7 reports the monthly and annual energy flows calculated using Equations 1 to 4. The outliers mainly occurred in June and July, so their respective energy flows are not presented.

Table 7. Monthly and annual energy flows for solar energy supplied, domestic hot water, space heating, and thermal energy stored for the year 2014

	Measurements [kWh]				Predictions [kWh]			
Month	Q_{supply}	Q_{DHW}	Q_{SH}	Q_{stored}	Q_{supply}	Q_{DHW}	Q_{SH}	Q_{stored}
January	297	144	0	153	382	202	0	180
February	1335	605	0	730	353	192	0	160
March	304	140	0	164	347	212	0	135
April	356	156	0	200	363	228	0	135
May	472	249	0	223	332	196	0	136
June	-	-	-	-	-	-	-	-
July	-	-	-	-	-	-	-	-
August	610	212	0	398	585	153	0	432
September	264	255	57	-48	268	208	42	18
October	159	215	30	-85	190	181	24	-14
November	253	125	223	-95	244	131	181	-68
December	179	130	199	-150	187	116	164	-94
Annual	3,197	1,754	509	934	3,252	1,820	409	1,022

CONCLUSIONS

A TRNSYS model validation of a residential solar thermal combisystem installed in Massachusetts, USA, was presented in this paper. A lack of standards for calibration criteria was pointed out. Results obtained showed that the measured temperatures were predicted with a NMBE and CVRMSE ranged from –-2.1% to 9% and from 8.6% to 25.1%, respectively. BPS models can play a key role in designing and optimizing solar thermal combisystems; however, the importance of the uncertainty analysis and validation should not be overlooked before drawing any conclusion.

ACKNOLEDGEMENTS

The authors would like to acknowledge the financial support received from Natural Sciences and Engineering Research Council of Canada, and from Faculty of Engineering and Computer Science of Concordia University.

REFERENCES

Abdalla N. (2013), 'Validated TRNSYS Model for Solar Assisted Space Heating System', *2013 1st International Conference & Exhibition on the Applications of Information Technology to Renewable Energy Processes and Systems*, Amman, Jordan 139-143.

ASHRAE (2002), *Guideline 14-2002: Measurement of Energy and Demand savings*, ASHRAE, Atlanta, Georgia.

ASHRAE (2013), *ASHRAE Handbook – Fundamentals*, ASHRAE, Atlanta, Georgia.

Attia S., Hamdy M., O'Brien W., and Carlucci S. (2013), 'Assessing gaps and needs for integrating building performance optimization tools in net zero energy buildings design', *Energy and Buildings*, 60 110-124.

Ayompe L.M., Duffy A., McCormack J., and Conlon M. (2011), 'Validated TRNSYS model for forced circulation solar water heating systems with flat plate and heat pipe evacuated tube collectors', *Applied Thermal Engineering*, 31 1536-1542.

Bornatico R., Hüssy J., Witzig A., and Guzzella L. (2013), 'Surrogate modeling for the fast optimization of energy systems', *Energy*, 57 653-662.

Bornatico R., Pfeiffer M., Witzig A., and Guzzella L. (2012), 'Optimal sizing of a solar thermal building installation using particle swarm', *Energy*, 41 31-37.

Coakley D., Raftery P., and Keane M. Witzig A. (2014), 'A review of methods to match building energy simulation models to measured data', *Renewable and Sustainable Energy Reviews*, 37 123-141.

De Wit S. and Augenbroe G. (2002), 'Analysis of uncertainty in building design evaluations and its implications', *Energy and Buildings*, 34 951-958.

Dickinson R., and Cruickshank C. (2011), 'REVIEW OF COMBINED SPACE AND DOMESTIC HOT WATER HEATING SYSTEMS FOR SOLAR APPLICATIONS', *Proceedings of the ASME 2011 5th International Conference on Energy Sustainability*, Washington, DC, USA, 205-211.

Duffie J.A., and Beckman W.A. (2006), *Solar Engineering of Thermal Processes*, John Wiley & Sons, Inc., Hoboken, NJ, USA.

Ellehauge, K. (2015), *European Solar Combisystems: Webpage for the European Alterner Programme Project*, Last accessed: November 19, 2015, http://www.elle-kilde.dk/altener-combi/index.htm

EVO (2007), *International performance measurement & verification protocol*, Efficiency Valuation Organisation (EVO).

Hang Y., Qu M., and Zhao F. (2012), 'Economic and environmental life cycle analysis of solar hot water systems in the United States', *Energy and Buildings*, 45 181-188.

Hugo A., Zmeureanu R., and Rivard. H. (2010), 'Solar combisystem with seasonal thermal storage', *Journal of Building Performance Simulation*, 3 255-268.

IEA (2013), *Transition to sustainable buildings: Strategies and opportunities to 2050*, Paris: IEA/OECD.

IEA (2015), *Solar Heating and Cooling Programme*, Last accessed: November 19, 2015, http://task26.iea-shc.org/

Kacan E. and Ulgen K. (2012), 'Energy analysis of Solar Combisystems in Turkey', *Energy Conversion and Management*, 64 378-386.

Kalogirou S.A. (2004), 'Environmental benefits of domestic solar energy systems', *Energy Conversion and Management*, 45 3075-3092.

Leckner M. and Zmeureanu R. (2011), 'Life cycle cost and energy analysis of a Net Zero Energy House with solar combisystem', *Applied Energy*, 88, 232-241.

MATLAB (2015), *The Language of Technical Computing*, Last accessed: November 19, 2015, http://www.mathworks.com/products/matlab/.

Mauthner F. and Weiss W. (2013), *Solar heat worldwide markets and contribution to energy supply 2011*, AEE INTEC.

Ng Cheng Hin J. and Zmeureanu R. (2014), 'Optimization of a residential solar combisystem for minimum life cycle cost, energy use and exergy destroyed', *Solar Energy*, 100, 102-113.

Nyboer J. and Lutes K. (2011), *A Review of Renewable Energy in Canada, 2009*, Canadian Industrial Energy End-use Data and Analysis Centre Simon Fraser University, Burnaby, BC

Polysun (2015), *Polysun simulation software*, Last accessed: November 19, 2015, http://www.velasolaris.com/english/home.html.

Reddy T.A. (2011), *Applied Data Analysis and Modeling for Energy Engineers and Scientists*, Springer, New York, USA.

Suter J-M., Weiss T., and Inäbnit J. (2000), *IEA SHC - TASK 26 Solar Combisystems in Austria, Denmark, Finland, France, Germany, Sweden Switzerland, the Netherlands and the USA – Overview*, Gleisdorf, Austria: AEE INTEC.

TESS (2012), *TESSLibs 17 Component Libraries for the TRNSYS Simulation Environment*, Tech. Rep. Volume 11, Thermal Energy System Specialists.

TRNSYS (2015), *TRNSYS: Transient System Simulation Tool*, Last accessed: November 19, 2015, http://www.trnsys.com/.

Weather Analytics (2015), *Weather Analytics – Get Weather Smart*, Last accessed: November 19, 2015, http://www.weatheranalytics.com/wa/.